The American Journal of Pathology, Vol. 172, No. 4, April 2008

DOI: 10.2353/ajpath.2008.070756

Epithelial and Mesenchymal Cell Biology

Age-Related Changes in Bone Morphology Are Accelerated in Group VIA Phospholipase A_2 (iPLA$_2\beta$)-Null Mice

Sasanka Ramanadham,* Kevin E. Yarasheski,* Matthew J. Silva,† Mary Wohltmann,* Deborah Veis Novack,‡ Blaine Christiansen,† Xiaolin Tu,‡ Sheng Zhang,* Xiaoyong Lei,* and John Turk*

From the Medicine Department, Mass Spectrometry Facility, and Division of Endocrinology, Metabolism, and Lipid Research, and the Departments of Orthopaedic Surgery‡* and Medicine,‡ *Division of Bone and Mineral Diseases, Washington University School of Medicine, St. Louis, Missouri*

Phospholipases A_2 (PLA_2) hydrolyze the *sn*−2 fatty acid substituent, such as arachidonic acid, from phospholipids, and arachidonate metabolites are recognized mediators of bone modeling. We have previously generated knockout (KO) mice lacking the group VIA PLA_2 (iPLA$_2\beta$), which participates in a variety of signaling events; iPLA$_2\beta$ mRNA is expressed in bones of wild-type (WT) but not KO mice. Cortical bone size, trabecular bone volume, bone mineralizing surfaces, and bone strength are similar in WT and KO mice at 3 months and decline with age in both groups, but the decreases are more pronounced in KO mice. The lower bone mass phenotype observed in KO mice is not associated with an increase in osteoclast abundance/activity or a decrease in osteoblast density, but is accompanied by an increase in bone marrow fat. Relative to WT mice, undifferentiated bone marrow stromal cells (BMSCs) from KO mice express higher levels of PPAR-γ and lower levels of Runx2 mRNA, and this correlates with increased adipogenesis and decreased osteogenesis in BMSCs from these mice. In summary, our studies indicate that age-related losses in bone mass and strength are accelerated in iPLA$_2\beta$-null mice. Because adipocytes and osteoblasts share a common mesenchymal stem cell origin, our findings suggest that absence of iPLA$_2\beta$ causes abnormalities in osteoblast function and BMSC differentiation and identify a previously unrecognized role of iPLA$_2\beta$ in bone formation. ***(Am J Pathol 2008, 172:868–881; DOI: 10.2353/ajpath.2008.070756)***

Bioactive arachidonic acid (AA) metabolites (eicosanoids) generated by the actions of various oxygenases, such as the 5-lipoxygenase (5-LO) and cyclooxygenase (COX) isozymes, are important mediators of bone remodeling. The 5-LO products leukotrienes and 5-HETE (hydroxyeicosatetraenoic acid) function as negative modulators of bone formation by inhibiting osteoblast differentiation and bone formation.[1] In contrast, prostaglandins (PGs), eg, PGE_2, derived from COX metabolism of AA enhance bone formation and mass by increasing osteoblast replication and differentiation and/or by inhibiting osteoclastic resorption,[2–5] although high concentrations of PGE_2 can stimulate bone resorption.[6] Dietary supplementation with AA results in increases in bone mass and volume,[7,8] reflecting a beneficial role of eicosanoids in bone formation.

Most cellular AA is esterified in the *sn*−2 position of membrane glycerophospholipids and is inaccessible to 5-LO or COX.[9] Phospholipases A_2 (PLA_2s) are a diverse group of enzymes[10] that catalyze the hydrolysis of *sn*−2 fatty acid substituents to yield a free fatty acid, eg, AA, that can be converted to various eicosanoids.[11] PLA_2s are classified into 15 different groups on the basis of Ca^{2+} requirement and sequence homology. These include the low molecular weight secretory (s)PLA_2s, the group IV cytosolic (c)PLA_2s, and the group VI Ca^{2+}-independent (i)PLA_2s, among others.

The group VIA iPLA$_2$, designated iPLA$_2\beta$, is an 84- to 88-kDa cytosolic PLA_2 that does not require Ca^{2+} for catalysis, and its amino acid sequence includes eight N-terminal ankyrin repeats, a caspase-3 cleavage site, an ATP binding domain, a serine lipase consensus sequence (GXSXG), a bipartite nuclear localization sequence, and C-terminal calmodulin binding domain(s).[12] It has been proposed that iPLA$_2\beta$ participates in phos-

Supported by the National Institutes of Health (grants R01-DK69455, R37-DK34388, R01-AR47867, R01-AR052705, R01 DK049393, R01 DK059531, P41-RR00954, P60-DK20579, and P30-DK56341).

Accepted for publication December 18, 2007.

Address reprint requests to Sasanka Ramanadham, Ph.D., Washington University School of Medicine, Department of Internal Medicine, 660 S. Euclid Ave., Box 8127, St. Louis, MO 63110. E-mail: sramanad@im.wustl.edu.

pholipid remodeling, signal transduction, cell proliferation, and apoptosis.[12]

We have generated iPLA$_2\beta$-null mice by homologous recombination, and these mice exhibit defective spermatozoa motility,[13] pancreatic islet insulin secretion,[14] and signaling in macrophages.[15] iPLA$_2\beta$ mRNA is expressed in a wide variety of wild-type (WT) tissues[13] including bone marrow and spinal cord.[16] Here, we used 1) dual-energy X-ray absorptiometry (DEXA) scanning to determine bone mineral density (BMD), 2) microcomputed tomography (μCT) analyses to assess cortical and trabecular bone morphology, 3) whole-bone mechanical testing to examine bone strength, 4) histomorphometry to examine osteoclasts and osteoblasts, 5) calcein labeling to assess dynamic bone formation, 6) real-time polymerase chain reaction (PCR) to determine expression of adipogenic and osteogenic transcriptional factors, and 7) *ex vivo* differentiation of bone marrow progenitor cells into bone-forming cells or adipocytes in WT and iPLA$_2\beta$-null female mice. Our findings indicate that iPLA$_2\beta$ is expressed in normal bone and that iPLA$_2\beta$-null mice exhibit accelerated aging-related bone loss.

Materials and Methods

Materials

The reagents (and sources) used in these studies included: pentobarbital (Abbott Laboratories, Chicago, IL); FSH RIA kit (Alpco Diagnostic, Salem, NH); amylin EIA kit (Bachem CA Inc., Torrance, CA); osteocalcin EIA kit (Biomedical Technologies, Inc., Stoughton, MA); estradiol EIA kit (Cayman Chemical Co., Ann Arbor, MI); paraformaldehyde (Electron Microscopy Studies, Hatfield, PA); calcein, agarose, and SuperScript reverse transcriptase (Invitrogen, Carlsbad, CA); CTX EIA kit (Nordic Bioscience, Chesapeake, VA), ascorbic acid, β-glycerophosphate, diethlypyrocarbonate, and ethylenediaminetetraacetic acid (Sigma, St. Louis, MO); α-MEM and streptomycin (Mediatech Inc., Herndon, VA); and phosphate-buffered saline (PBS) (Tissue Culture Support Center, Washington University, St. Louis, MO).

Generation of iPLA$_2\beta^{-/-}$ Knockout Mice and iPLA$_2\beta$ mRNA Expression in Bones and Bone-Modeling Cells

The iPLA$_2\beta$-null mice were generated and genotyped, as described.[13,14] Briefly, 129SvJ embryonic stem cell clones containing the disrupted iPLA$_2\beta$ were injected into C57BL/6 mouse blastocysts, which were implanted into pseudo-pregnant females for gestation to yield chimeras. The chimeras were mated with WT C57BL/6 females (obtained from Charles River Laboratories, Wilmington, MA) to yield heterozygotes. Mating of the heterozygous offspring with each other produced iPLA$_2\beta^{-/-}$, iPLA$_2\beta^{-/+}$, and iPLA$_2\beta^{+/+}$ in a 1:2:1 ratio. The female wild-type (iPLA$_2\beta^{+/+}$, WT) littermates of iPLA$_2\beta$-null (iPLA$_2\beta^{-/-}$, KO) mice produced by heterozygous breeding pairs were used as controls. The animals were maintained with free access to food (Purina Lab Diet; El-Mel, St. Louis, MO) and water, five per cage, under alternating 12-hour light/dark cycles. The Washington University Animal Studies Committee (St. Louis, MO) approved all studies.

To examine the presence of iPLA$_2\beta$ in bones, both sets of femora and tibiae were isolated from 3-month-old WT and iPLA$_2\beta$-null female mice. One set of bones containing marrow cells from each mouse was frozen immediately in liquid nitrogen. The marrow cells were flushed out of the second set of bones from each mouse with cold PBS containing 0.10% diethyl-pyrocarbonate to inhibit RNases before freezing. The frozen bones were pulverized using a precooled Bessman tissue pulverizer (Spectrum Chemical Laboratory Products, Gardena, CA) and total RNA was prepared from 100 mg of bone powder using the Trizol method as described[17] and cDNA templates were generated with SuperScript reverse transcriptase. PCR primers were generated based on sequences in the GenBank data base and the primer sets and expected bp product sizes were: iPLA$_2\beta$ (accession no. BC003487), sense 5′-TTTCAGTCATGGCATCCAGT-3′ and antisense 5′-TATGCGTGGTGTGTACTTCCG-3′ (400 bp), and internal standard 18S (K01364), sense 5′-CGCTTCCTTACCTGGTTGAT-3′ and antisense 5′-TCCCTCTCCGGAATCGAA-3′.[13,14] PCR products were analyzed by 1% agarose gel electrophoresis and visualized by ethidium bromide staining. In addition, to examine cellular localization of iPLA$_2\beta$, its message expression was determined in murine calvarial osteoblasts and osteoclasts, prepared as described.[18,19]

Whole Body Composition Analyses by DEXA and Plasma Analyses

Mice (3 months, 1 year, and 2 years of age) were anesthetized with pentobarbital (40 mg/kg, i.p.) and body weight (BW) and BMD measurements were obtained by DEXA (Lunar, Madison, WI) scanning. Estradiol, amylin, osteocalcin, and CTX levels were measured by enzyme-linked immunosorbent assay, follicle-stimulating hormone by radioimmunoassay, and creatinine and blood urea nitrogen by spectrophotometry using a dry-chemistry reaction.

Microcomputed Tomography (μCT) Analyses of Cortical and Trabecular Bone

Femora and L4 vertebrae were isolated from WT and iPLA$_2\beta$-null (KO) female mice to assess cortical and trabecular bone parameters, respectively, by μCT. Isolated bones were suspended in agarose (1.5%) and scanned using a conebeam μCT scanner (model μCT 40; Scanco, Bassersdorf, Switzerland), as described (X-ray energy, 55 KEV; intensity, 145 μA; integration time, 150 ms; resolution, 16 μm, threshold, 300).[20] Cortical bone morphology was assessed at a region spanning 3 mm, centered at the mid-diaphysis of the femur. Three transverse slices (16 μm/slice) were obtained at four locations: 0.5 and 1.5

mm proximal and distal from the mid-diaphysis. Using image processing software (ImageJ; National Institutes of Health, Bethesda, MD) and custom Excel (Microsoft, Redmond, WA) macros, we determined cortical bone area, moments of inertia about the *x*- and *y*-axes (where the *x* axis is aligned with the medial-lateral direction) and average cortical thickness. Results were averaged over the 12 slices. Trabecular bone analyses were done throughout the entire length of the L4 vertebra. The vertebral body starting immediately adjacent to the caudal endplate region was selected for analyses using contours inside the cortical shell on each two-dimensional image. Trabecular (Tb) bone volume relative to total bone volume (TbBV/TBV), number ($Tb.N^{+}$), thickness ($Tb.Th^{+}$), and spacing ($Tb.Sp^{+}$) were determined using the manufacturer's three-dimensional analysis tools ($^{+}$denotes the direct method of calculation, not based on stereological models).

Whole-Bone Mechanical Testing

Mechanical testing of intact femora was done by three-point bending as previously described.[21] Specimens were thawed, soaked in saline for 1 hour before testing to ensure hydration, and were tested at room temperature using a servohydraulic-testing machine (1331/8500R; Instron, Norwood, MA). Bones were placed with their anterior side down on two horizontal supports spaced 7 mm apart; the central loading point contacted the posterior surface of the diaphysis at the midpoint of the bone length. The loading point was displaced downward (transverse to the long axis of the bone) at 0.03 mm/second until failure, generating bending in the anteroposterior plane. Load-displacement data were recorded at 60 Hz (Labview; National Instruments, Austin, TX) and test curves were analyzed to determine measures of whole-bone strength (ultimate moment), bending moment when the bone starts to fail (yield moment), stiffness (rigidity), ductility (post-yield displacement), and resistance to fracture (energy-to-fracture).

Osteoclast and Osteoblast Measures

Tibiae were obtained from 3- and 6-month-old WT and KO mice, fixed overnight in paraformaldehyde (4%), and embedded in paraffin for osteoclast and osteoblast analyses. Longitudinal sections (10 μm thickness) of the tibiae were prepared and TRAP stain was used to visualize osteoclasts and hematoxylin and eosin (H&E) stain to visualize osteoblasts. Osteoclast measures were determined in a 600-μm field across the bone that was one field distal to the growth plate and analyzed using commercial software (Osteomeasure; OsteoMetrics, Decatur, GA). Quantitated measures included osteoclast number/bone perimeter (N.Oc/B.Pm) and osteoclast surface/bone surface (Oc.S/BS). Osteoblasts lining the endocortical bone surface were counted and osteoblast number in the 1000- to 4000-μm region from the growth plate, relative to bone surface (Ob.N/mm), was analyzed by Osteomeasure software. Images were captured using a Coolpix camera (Nikon, Tokyo, Japan).

Dynamic Bone Formation Analyses by Calcein Labeling

To compare the dynamic rate of bone formation in WT and KO mice, 3- and 6-month-old female mice were injected two times with calcein (7.5 mg/kg, i.p.) 10 days apart. BWs at both 3 months (WT, 22.7 $\pm$ 0.5 g and KO, 21.5 $\pm$ 0.5 g; $P = 0.1145$) and 6 months (WT, 24.9 $\pm$ 0.8 g and KO, 26.1 $\pm$ 0.8 g; $P = 0.3188$) were similar in the two groups. The animals were sacrificed on day 12, and undecalcified bones were embedded in methyl methacrylate. Longitudinal sections (10 μm thickness) of the tibiae were then prepared and new bone formation was assessed by fluorescence microscopy of calcein green using a fluorescein isothiocyanate filter. Endosteal and periosteal bone measures were taken along a 1000- to 4000-μm region from the growth plate. Dynamic measurements were determined using Osteomeasure software and included mineral apposition rate (MAR) in the trabeculae (Tb.MAR), and MAR, percent single(sLS/BS)- and double (dLs/BS)-labeled bone surface, total mineralizing surface (MS/BS), and bone formation rate (BFR/BS) at the endocortical (Ec) and periosteal (Ps) surfaces.

H&E Staining

Tibiae from WT and KO female mice were isolated and fixed overnight in paraformaldehyde (4%), decalcified throughout 1 week, embedded in paraffin, and sectioned longitudinally (10-μm-thick slices) for H&E staining. The sections were examined for changes in the bone marrow and staining was visualized with a Nikon SMZ800 microscope and images captured using a Nikon Coolpix camera.

iPLA$_2\beta$, PPARγ, and Runx2 Message Expression in BMSCs

Primary cultures of the BMSCs, containing progenitor cells for bone and adipocyte formation, were isolated from the femur and the tibia of 3-month-old WT and KO female mice, as described[22] with slight modification. Briefly, on surgical removal of the epiphyseal ends, the bone shafts were flushed with α-MEM with a 25-gauge needle. Cells from a single mouse were centrifuged, treated with 1 ml of red blood cell lysis buffer (Roche, Mannheim, Germany) for 5 minutes, rinsed, and resuspended in α-MEM containing 20% fetal bovine serum, filtered through a 70-μm cell strainer, and plated at 2×10^6/well in 12-well plates. Half of the medium was changed at day 3 and all medium changed at day 6 of culture to remove floating cells. On day 10, the cells were harvested and total RNA was prepared, as described above, for real-time PCR analyses of iPLA$_2\beta$, *PPAR*γ, and *Runx2* messages. Isolated RNA was treated with DNase (Invitrogen) before cDNA synthesis. The sense/antisense primer sets were as follows: iPLA$_2\beta$, sense 5′-GCCCTGGCCATTCTACACAGTA-3′ and antisense 5′-CACCTCATCCTTCATACGGAAGT-3′; *PPAR*γ, sense 5′-CACAATGCCATCAGGTTTGG-3′ and antisense 5′-GCTGGTC-

GATATCACTGGAGATC-3′; *Runx2*, sense 5′-CCGTGGC-CTTCAAGGTTGT-3′ and antisense 5′-TTCATAACAGC-GGAGGCATTT-3′; and 18S control, sense 5′-AGTCCT-GCCCTTTGTACACA-3′ and antisense 5′-GATCCGA-GGGCCTCACTAAAC-3′.

Induction of Osteogenesis and Adipogenesis in BMSC Cultures

Primary cultures of BMSCs were prepared and cultured as above for 10 days. The media was then switched to a mineralization media containing 50 μg/ml of ascorbic acid and 50 mmol/L β-glycerophosphate and bone nodule formation was visualized using von Kossa stain.[23] For adipogenesis assay, the media was switched to a medium containing 0.5 mmol/L IBMX, 60 mmol/L indomethacin, and 0.5 mmol/L hydrocortisone and adipogenesis was assessed by lipid droplet accumulation in cells.[24]

Data Analysis

Data were converted to mean ± SEM and significant differences ($P < 0.05$) between WT and KO mice were analyzed by unpaired Students' *t*-test or by analysis of variance with appropriate post hoc tests. Age-related changes in each group were determined by calculating the difference between values at a given age from the mean values in 3-month-old mice with the same genotype.

Results

Demonstration of Presence of iPLA$_2\beta$ mRNA in Bones of WT Mice and Its Absence in Those of iPLA$_2\beta$-Null Mice by PCR

Heterozygous (iPLA$_2\beta^{+/-}$) breeding pairs yielded a Mendelian ratio of WT (iPLA$_2\beta^{+/+}$), knockout (KO, iPLA$_2\beta^{-/-}$), and heterozygous progeny. All mice used in this study were genotyped using Southern analyses, as described.[13] To determine whether bones contain iPLA$_2\beta$, expression of iPLA$_2\beta$ message in the femur and tibia isolated from WT and iPLA$_2\beta$-null mice was analyzed by PCR. An expected PCR product of size 400 bp is generated from bone cDNA templates prepared from WT mice (Figure 1), and the intensity of iPLA$_2\beta$ message in the absence or presence of bone marrow cells is found to be similar. In contrast, no PCR product is generated from bone cDNA templates prepared from KO mice, indicating that bones in WT mice express iPLA$_2\beta$ mRNA and that it is absent in bones of iPLA$_2\beta$-null mice. PCR analyses also demonstrate iPLA$_2\beta$ mRNA expression in murine calvarial osteoblasts (Figure 2) and real-time PCR analyses reveal that the calvarial osteoblasts express a twofold higher ($P < 0.0001$) message for iPLA$_2\beta$ than cultured osteoclasts. These findings indicate that iPLA$_2\beta$ mRNA is expressed in bone-modeling cells from WT mice and is absent in bones from KO mice.

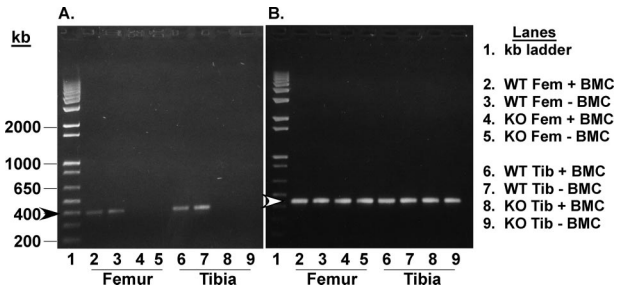

Figure 1. iPLA$_2\beta$ message expression in femora and tibiae of WT and iPLA$_2\beta$-null mice. RT-PCR analyses were performed on RNA from bone without and with bone marrow, and iPLA$_2\beta$ (**A**) and 18S rRNA (**B**) PCR products were visualized by ethidium bromide staining. **Arrowheads** indicate the expected PCR products of iPLA$_2\beta$ (dark, 400 bp) and 18S rRNA (light, 450 bp).

Whole Body Composition Analyses by DEXA

To compare whole body composition throughout time, WT and iPLA$_2\beta$-null mice were subjected to DEXA scanning at the ages of 3 months, 1 year, and 2 years. As illustrated in Figure 3, BW (Figure 3A) and BMD (Figure 3B) of KO mice are similar to WT mice at 3 months but are decreased at 1 and 2 years, relative to age-matched WT mice. Both parameters increased in WT at 1 year, relative to 3 months ($P < 0.05$), and did not change further at 2 years. In contrast, KO mouse BW increased between 3 months and 1 year but decreased to 3-month levels by 2 years and BMD did not change during the entire 2-year study period. These findings raise the possibility that normal bone development is affected in the absence of iPLA$_2\beta$.

Cortical Bone Area and Moment of Inertia Decrease in KO Mice with Age

To determine whether cortical bone is abnormal in mice that lack iPLA$_2\beta$, femora were collected from WT and KO mice and cortical bone was analyzed at the mid-diaphysis using microcomputed tomography (μCT). Cortical bone area (CrB.Ar), and medial-lateral (Ixx) and anteroposterior (Iyy) moments of inertia in bone from the 3-month-old WT and KO mice are similar and increase during the first year in both groups by comparable amounts (Table 1). WT mice show a progressive increase in bone area and moments of inertia with aging (Figure 4A and Table 1), but these parameters fail to increase in KO mice. These findings suggest that cor-

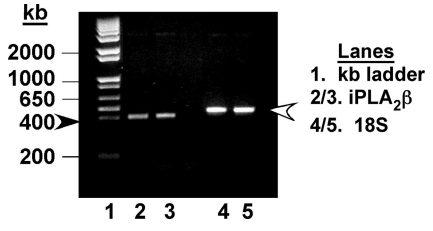

Figure 2. iPLA$_2\beta$ message expression in osteoblasts. Total RNA was prepared from 7-day differentiated murine calvarial osteoblast-forming cells and RT-PCR reactions and visualization of iPLA$_2\beta$ message were done as in Figure 1. **Arrowheads** indicate the expected PCR products of iPLA$_2\beta$ (dark, 400 bp) and 18S (light, 450 bp).

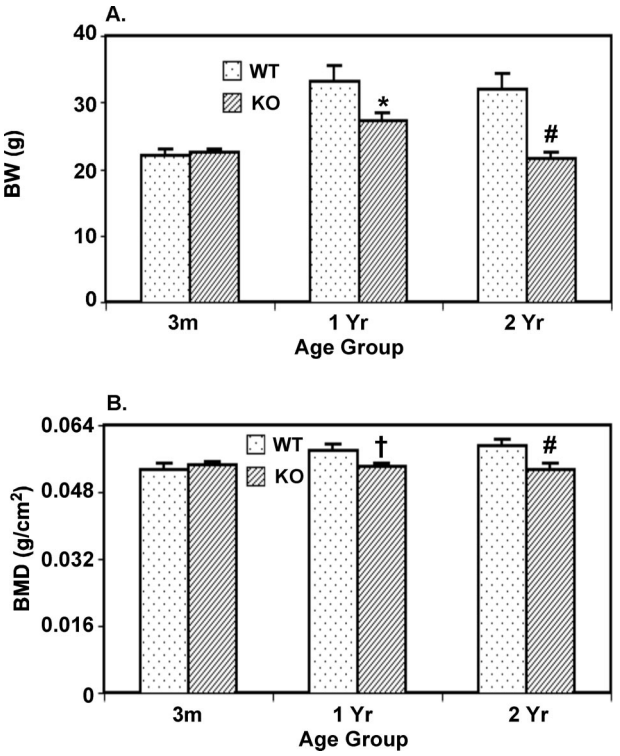

Figure 3. Comparison of BW and BMD in WT and iPLA$_2\beta$-null mice by DEXA scanning. Mice were anesthetized with pentobarbital (40 mg/kg, i.p.) and BW and areal whole-body BMD were measured by DEXA scanning. The data represent mean ± SEM, where $n = 7$ to 12 at each age. KO group significantly different from age-matched WT group, $^*P < 0.05$, $^\#P < 0.005$, and $^\dagger P < 0.0001$, respectively.

tical bone development is impaired in iPLA$_2\beta$-null mice.

Whole-Bone Mechanical Testing Reveals Decreases in Cortical Bone Strength in KO Mice with Age

We next examined whether diminished BMD and CrB.Ar with aging are associated with greater fragility of KO bones; whole-bone mechanical testing with 3-point bending was performed on femora. At 3 months, there are no differences between the WT and KO mice in ultimate moment, yield moment, postyield displacement/gauge factor, rigidity, and energy to fracture. Between 3 months and 1 year, ultimate moment, yield moment, and R increase and postyield displacement and energy to fracture decrease in both WT and KO mice (Table 1) and the magnitude of changes are not statistically different between the two groups. In contrast, while the measures of whole-bone strength (ultimate moment), bending moment at onset of bone failure (yield moment), whole-bone stiffness (rigidity), ductility (post-yield displacement), and resistance to fracture (energy to fracture) are unchanged in the WT mice between 1 and 2 years, all parameters, except post-yield displacement/gauge factor, are reduced in the KO mice during this period. Taken together, these findings indicate that bones from iPLA$_2\beta$-null mice have similar mechanical properties as WT bones up to 1 year of age, but are less strong and more fragile than WT bones at 2 years.

Trabecular Bone Density Decreases in KO Mice with Age

To determine whether trabecular bone development is also affected in iPLA$_2\beta$-null mice, μCT analyses were performed along the entire length of L4 vertebrae isolated from the WT and KO mice. Construction of a frontal plane section (96 μm) image of vertebrae reveals a dense trabecular network in both groups at 3 months, especially near the endplates (Figure 4B). Although the trabecular network remains intact in the WT mice with age, signs of deterioration are apparent at 1 year in the KO mice (data not shown). By 2 years, there is a dramatic loss in trabeculae of KO mice. The trabecular network was examined throughout a range of cross-sections, and three-dimensional analyses were then used to determine trabecular morphological parameters (Table 2). At 3 months of age, these trabecular measures are similar in the WT and KO mice. In the WT mice, they do not change significantly with age, although Tb.BV/TBV and Tb.N$^+$ tend to be lower and Tb.Sp$^+$ higher in the 2-year mice, relative to 3-month WT mice. In contrast, Tb.BV/TBV in KO mice at 1 and 2 years is significantly lower than in age-matched WT

Table 1. Cortical Bone Assessment in WT and iPLA$_2\beta$-Null Mice by μCT and Whole Bone Mechanical Strength Testing

Trabecular measurement	3-Month WT	3-Month KO	1-Year WT	1-Year KO	2-Year WT	2-Year KO
Bone area (mm^2)	0.82 ± 0.04	0.89 ± 0.02	0.96 ± 0.05	1.04 ± 0.08	1.10 ± 0.02	0.88 ± 0.03‡
Ixx (mm^4)	0.10 ± 0.01	0.13 ± 0.01	0.17 ± 0.02	0.19 ± 0.02	0.28 ± 0.01	0.20 ± 0.01†
Iyy (mm^4)	0.21 ± 0.02	0.24 ± 0.01	0.27 ± 0.02	0.32 ± 0.04	0.34 ± 0.02	0.28 ± 0.05
Average thickness (mm)	0.42 ± 0.04	0.38 ± 0.04	0.24 ± 0.01	0.31 ± 0.02*	0.26 ± 0.02	0.21 ± 0.02
Ultimate moment (Nmm)	30.76 ± 2.08	35.39 ± 0.09	49.01 ± 3.21	44.85 ± 3.91	50.42 ± 4.20	34.48 ± 3.25*
Yield moment (Nmm)	23.91 ± 1.96	26.11 ± 1.35	32.03 ± 5.30	34.71 ± 4.35	32.52 ± 2.22	22.94 ± 3.55*
Post-yield displacement/ gage factor (mm/mm^2)	0.18 ± 0.05	0.15 ± 0.04	0.08 ± 0.01	0.05 ± 0.01*	0.05 ± 0.01	0.04 ± 0.01
Rigidity [Nmm/(mm/mm^2)]	809 ± 21	833 ± 66	1300 ± 91	1090 ± 86	1329 ± 90	847 ± 140*
Energy to fracture [Nmm*/ (mm/mm^2)]	4.02 ± 0.64	4.66 ± 0.86	3.90 ± 0.48	2.91 ± 0.31	3.30 ± 0.56	1.75 ± 0.37*

Femora were isolated from mice for analyses of bone area and whole bone mechanical testing by three-point bending. Ixx and Iyy, moments of inertia about the x- and y-axes. Displacement data are normalized by gage factor.[21]. The data represent mean ± SEM, where $n = 7$ to 9 each in the 3-month and 1-year groups and 3 to 5 each in the 2-year groups.*†‡KO group significantly different from age-matched WT group, $P < 0.001$, $P < 0.005$, $P < 0.05$.

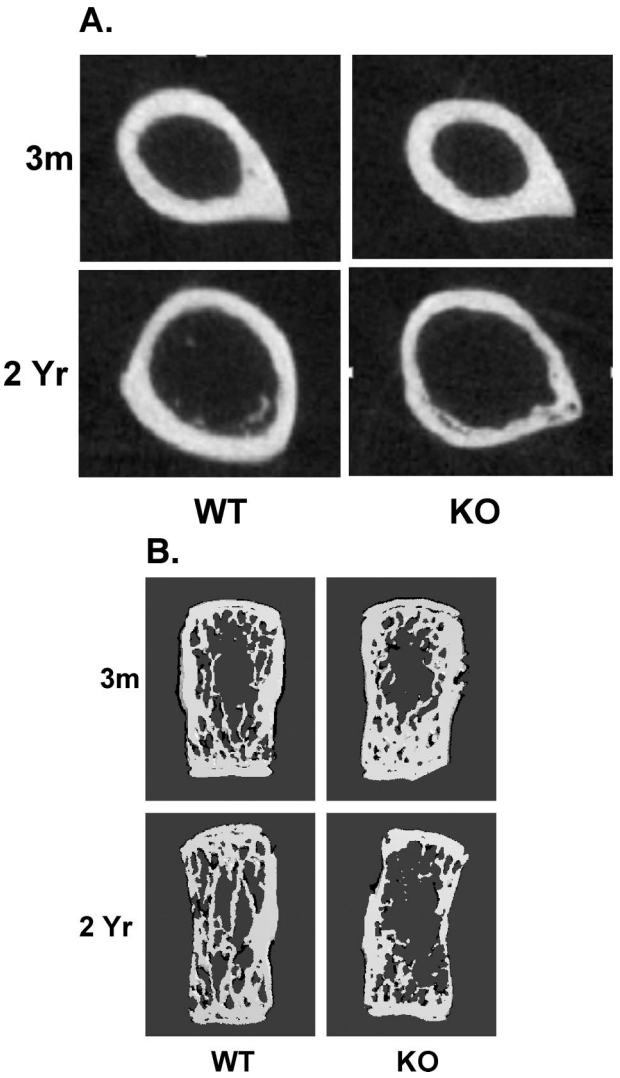

Figure 4. Analyses of femoral cortical bone and L4 vertebral trabecular bone of WT and iPLA$_2\beta$-null mice by μCT. Femora and L4 vertebrae from mice were used to examine cortical and trabecular bone morphology by μCT analyses. **A:** Transverse sections of femora at mid-diaphysis. **B:** Frontal plane sections (96 μm) of L4 vertebrae.

mice and is decreased by nearly 40% and 70%, respectively, relative to 3-month KO mice. Tb.N$^+$ in KO mice at 1 and 2 years is also significantly decreased, relative to age-matched WT mice, and by 2 years the Tb.N$^+$ is reduced by 55%, relative to 3-month KO mice. Although Tb.Th$^+$ is unchanged with age in the KO mice, Tb.Sp$^+$ at 2 years is significantly higher than in the 3-month mice. These findings reveal that, similar to cortical bone, there is an age-related loss of trabecular bone in iPLA$_2\beta$-null mice that is greater than normal.

Osteoclast Density Is Not Increased in KO Mice

Because increased bone resorption may be a cause of losses in bone volume in KO mice, TRAP-stained sections of tibiae were used to identify and quantitate osteoclasts, which stain red (Figure 5A). No significant differences in osteoclast number are evident with age in either WT or KO mice, except that, Oc.S/BS is decreased more in the KO, relative to age-matched WT mice (Table 3). Further, plasma levels of C-terminal telopeptide of type I collagen (CTX), a marker for bone resorption, are similar between the two groups (Table 4). These findings indicate that increases in osteoclast number or activity are not responsible for the lower bone volumes in iPLA$_2\beta$-null mice.

Osteoblast Density Is Similar in KO Mice

Next, the possibility that the low bone mass phenotype in KO mice is related to changes in osteoblast density was examined using H&E stain to identify and quantitate mononucleated osteoblast cells lining the endosteal bone. Quantitation of cell abundance using Osteomeasure software reveal no significant differences in 3-month animals (Table 3). At 6 months, the osteoblast number/mm bone surface decreases in both groups, relative to 3 months. However, there was no significant difference between the WT and KO groups at 6 months. These findings suggest that the lower bone volumes in iPLA$_2\beta$-null mice cannot be attributed to a decrease in the abundance of bone-forming cells.

Calcein Labeling Demonstrates an Accelerated Decrease in Bone Formation in KO Mice with Age

Because decreased osteoblast function might also contribute to lower bone mass in the iPLA$_2\beta$-null mice, mineralizing bone surfaces in the WT and KO mice were assessed using calcein to fluorescently label active bone-forming surfaces. Two doses of calcein were administered 10 days apart to 3- and 6-month-old mice, and the distance between the two surfaces reflecting the MAR

Table 2. Morphometrics of L4 Trabeculae from WT and iPLA$_2\beta$-Null Mice by μCT Analyses

Trabecular measurement	3-Month WT	3-Month KO	1-Year WT	1-Year KO	2-Year WT	2-Year KO
Tb.BV/TBV (%)	34.6 ± 4.6	49.4 ± 6.9	43.2 ± 6.7	30.6 ± 3.4*†	29.3 ± 3.8	15.4 ± 0.6*†
Tb.N$^+$	6.92 ± 1.31	6.96 ± 0.71	6.39 ± 0.11	5.76 ± 0.10*	5.16 ± 0.74	3.16 ± 0.73*†
Tb.Th$^+$ (mm)	0.073 ± 0.004	0.089 ± 0.007	0.085 ± 0.009	0.082 ± 0.006	0.079 ± 0.004	0.070 ± 0.008
Tb.Sp$^+$ (mm)	0.171 ± 0.030	0.146 ± 0.023	0.144 ± 0.008	0.152 ± 0.025	0.236 ± 0.038	0.331 ± 0.036†

L4 vertebrae were isolated from mice and used to determine trabecular bone parameters by μCT analyses. Trabecular (Tb) bone volume relative to total bone volume (Tb.BV/TBV), number (Tb.N$^+$), thickness (Tb.Th$^+$), and spacing (Tb.Sp$^+$) were determined using the manufacturer's three-dimensional analysis tools. The data represent mean ± SEM, where n = 7 to 9 each in the 3-month and 1-year groups and 3 to 5 each in the 2-year group. *KO group significantly different from age-matched WT group at $P < 0.05$. †Two-year KO group significantly different from 3-month KO group, $P < 0.05$.

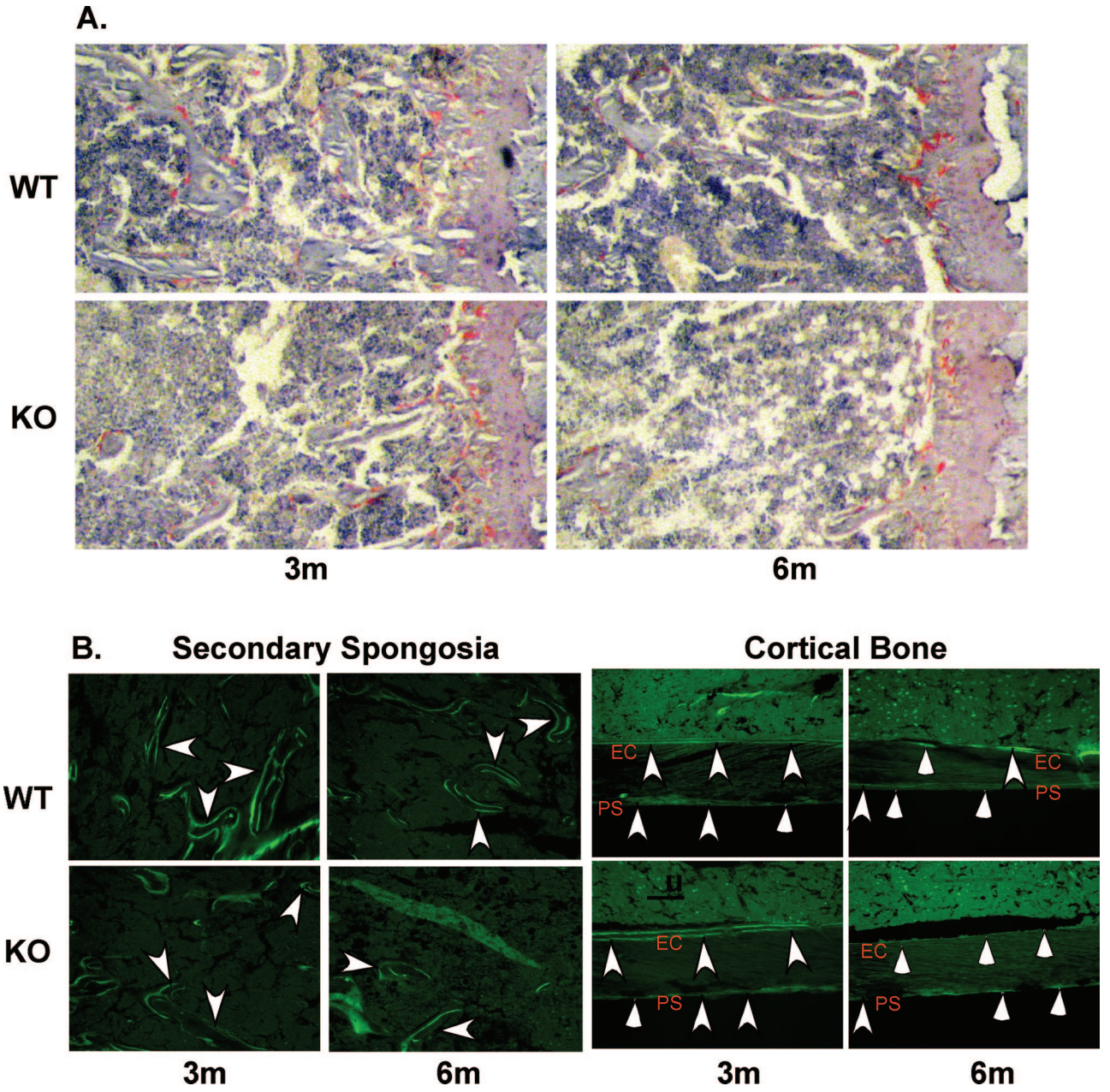

Figure 5. Histological assessment of bone properties in WT and iPLA$_2\beta$-null mice by μCT. **A:** TRAP staining. Longitudinal sections (10 μm) of undecalcified tibiae were stained with TRAP. Osteoclast (in red) measures were determined in a 600-μm field across the bone that was one field distal to the growth plate and analyzed using commercial software (Osteomeasure; OsteoMetrics, Decatur, GA). **B:** Calcein labeling. Longitudinal sections (10 μm) of undecalcified tibiae bone were obtained from calcein-administered mice and active bone formation, reflected by calcein green fluorescence, was visualized by fluorescence microscopy using a fluorescein isothiocyanate filter. **Left:** Trabeculae labeling in the secondary spongiosa. **Right:** Endosteal and periosteal bone labeling. **Arrowheads** indicate double-labeled bone regions and **arrows** indicate single-labeled bone regions. Endosteal and periosteal bone measures were taken along a 1000- to 4000-μm region from the growth plate. Dynamic measurements were determined using Osteomeasure software. Ps, periosteal bone; Ec, endocortical bone. Original magnifications, $\times$10.

was measured. Analyses in the secondary spongiosa region of the bone reveal a decrease (Figure 5B) in the trabecular MAR (Tb.MAR) in the KO mice at both 3 and 6 months in the KO mice, relative to age-matched WT mice (3 months: WT, 1.34 $\pm$ 0.18 μm/day and KO, 0.96 $\pm$ 0.11 μm/day, $P = 0.0563$; and 6 months: WT, 1.27 $\pm$ 0.09 μm/day versus KO, 0.89 $\pm$ 0.06 μm/day, $P = 0.0109$). Analyses of the periosteal (Ps) and endocortical (Ec) surfaces reveal minimal or no differences between the two groups at 3 months (Table 3, Figure 5B). At 6 months, only Ps.MAR and Ps.BFR/BS are significantly reduced in the KO group, relative to age-matched WT group. In contrast, dramatic differences in the endocortical (Ec) bone of the two groups are evident at 6 months. Single-labeled bone surface (Ec.sLS/BS) is significantly increased in the KO mice, with an apparent absence in double-labeled bone surface (Ec.dLS/BS). In the WT mice, Ec.sLS/BS did not change and the Ec.BFR/BS decreased by nearly 60% between 3 months and 6 months. At 6 months, double labeling is evident at 27% of the Ec

Table 3. Evaluation of Osteoclasts, Osteoblasts, and Dynamic Histomorphometric Properties in WT and iPLA$_2\beta$-Null Mice by TRAP and H&E Stain, and Calcein Labeling

	3-Month WT	3-Month KO	6-Month WT	6-Month KO
Osteoclast measure				
N.Oc/B.Pm (no./mm)	13.90 ± 4.04	14.87 ± 2.22	15.03 ± 2.46	14.55 ± 2.03
Oc.S/BS (%)	25.11 ± 8.02	21.85 ± 3.85	24.24 ± 2.56	19.00 ± 0.27*
Osteoblast measure				
N.Ob/B.Pm (no./mm)	42.12 ± 2.68	41.90 ± 1.70	23.63 ± 1.39	20.09 ± 1.17
Periosteal bone (Ps)				
Ps.sLS/BS (%)	22.38 ± 7.03	26.51 ± 8.49	42.85 ± 3.39†	38.32 ± 1.99
Ps.dLS/BS (%)	31.48 ± 8.10	16.41 ± 5.73	10.03 ± 5.32	4.04 ± 2.95
Ps.MS/BS (%)	42.66 ± 4.93	29.67 ± 2.94*	31.46 ± 4.73	23.20 ± 3.80
Ps.MAR (μm/day)	0.94 ± 0.05	1.80 ± 0.50	0.84 ± 0.38	0.45 ± 0.27†
Ps.BFR/BS ($\mu m^3/\mu m^2$/day)	0.40 ± 0.05	0.53 ± 0.15	0.27 ± 0.10	0.12 ± 0.07†
Endocortical bone (Ec)				
Ec.sLS/BS (%)	18.81 ± 7.09	25.54 ± 8.99	17.73 ± 1.66	29.87 ± 6.07*
Ec.dLS/BS (%)	63.81 ± 12.23	50.54 ± 18.44	27.29 ± 5.46†	0.00 ± 0.00*†
Ec.MS/BS (%)	73.22 ± 8.89	63.56 ± 15.75	36.15 ± 4.64†	15.11 ± 4.28*†
Ec.MAR (μm/day)	1.26 ± 0.20	1.51 ± 0.38	1.02 ± 0.25	0.00 ± 0.00*†
Ec.BFR/BS ($\mu m^3/\mu m^2$/day)	0.93 ± 0.20	1.12 ± 0.52	0.40 ± 0.15	0.00 ± 0.00*†

Undecalcified tibiae sections were prepared and osteoclasts, osteoblasts, and mineralizing surfaces were visualized by TRAP staining, H&E staining, and calcein labeling, respectively. Osteomeasure software was used to quantitate the following: N, number; Oc, osteoclast; Ob, osteoblast; Ps, periosteal bone; Ec, endocortical bone; MAR, mineral apposition rate; sLS/BS and dLS/BS, percent single- and double- (dLs/BS) labeled bone surface; MS/BS, total mineralizing surface; BFR/BS, bone formation rate. The data represent mean ± SEM, where $n = 4$ to 6 in each group. *KO group significantly different from age-matched WT group, $P < 0.05$. †Six-month group significantly different from corresponding 3-month group, $P < 0.05$.

bone surface, suggesting continued new bone formation in the WT mice. In contrast, there is no double-labeled surface in the 6-month KO mice, resulting in a zero value for mineral apposition rate (Ec.MAR) and bone formation (Ec.BFR/BS). Ec.MS/BS is also significantly reduced in the 6-month KO mice, relative to age-matched WT group. Thus, periosteal and, more prominently, trabecular and endosteal bone formation are significantly decreased in iPLA$_2\beta$-null mice. The reduced MS/BS and MAR in KO mice therefore suggest that a decrease in osteoblast function contributes to the low bone mass phenotype in iPLA$_2\beta$-null mice.

Plasma Markers of Bone Modeling in WT and KO Mice

To explain the low bone mass phenotype in the iPLA$_2\beta$-null mice, we examined plasma levels of biomarkers for bone formation (osteocalcin) and resorption (CTX) and these are not found to be significantly different between the two groups (Table 4). Because recent reports suggest that fertility and stimulated insulin secretion are impaired in iPLA$_2\beta$ mice,[13,14] we examined plasma levels of known modulators of bone modeling; estradiol,[25] follicle-stimulating hormone,[26] and amylin,[27] which is co-secreted with insulin from β-cells. As shown in Table 4, plasma concentrations of estradiol and amylin in the KO and age-matched WT mice are not statistically different. Plasma follicle-stimulating hormone is also similar in the two groups at 3 months and 1 year but is higher in the WT group at 2 years. We next examined if renal function, which can also impact bone formation,[28] is abnormal in the absence of iPLA$_2\beta$. We, however, found that plasma levels of creatinine and blood urea nitrogen in the WT and KO groups are well within the normal ranges expected for mice. These findings suggest that typical circulating factors or renal function that can impact bone modeling are not dysregulated in the KO mice.

Fat Accumulates in Bone Marrow of KO Mice with Age

In confirmation of μCT analyses, a greater reduction in tibial trabeculae from KO mice, relative to age-matched

Table 4. Comparison of Renal Function and of Factors that Can Affect Bone Modeling in WT and iPLA$_2\beta$-Null Mice

Measurement	3-Month WT	3-Month KO	6-Month WT	6-Month KO	1-Year WT	1-Year KO	2-Year WT	2-Year KO
Osteocalcin (ng/ml)	69 ± 5	80 ± 8	44 ± 10	52 ± 5	nd	nd	nd	nd
CTX (ng/ml)	24 ± 3	25 ± 3	17 ± 3	16 ± 2	nd	nd	nd	nd
Estradiol (pg/ml)	6.6 ± 0.9	7.4 ± 2.0	nd	nd	13.4 ± 3.2	7.4 ± 1.2	5.2 ± 0.9	7.7 ± 2.1
FSH (ng/ml)	8.4 ± 2.0	9.7 ± 1.6	nd	nd	9.4 ± 2.0	8.9 ± 1.1	18.4 ± 2.3	8.5 ± 0.3*
Amylin (ng/ml)	0.13 ± 0.01	0.14 ± 0.02	nd	nd	0.12 ± 0.01	0.11 ± 0.00	0.11 ± 0.01	0.10 ± 0.01
Creatinine (mg/dl)	0.39 ± 0.01	0.55 ± 0.10	0.54 ± 0.10	0.50 ± 0.10	0.38 ± 0.02	0.40 ± 0.0	nd	nd
BUN (mg/dl)	18 ± 2	13 ± 1	12 ± 2	19 ± 2	12 ± 2	17 ± 2	nd	nd

Blood was collected from 3-month, 6-month, 1-year, and 2-year WT and iPLA$_2\beta$-null mice. Subsequently, plasma levels of estradiol, amylin, osteocalcin, and CTX were measured by ELISA, follicle-stimulating hormone (FSH) by RIA, and creatinine and BUN by spectrophotometry. The data represent mean ± SEM, where $n = 5$ to 10 at 3 months, 6 months, and 1 year and $n = 4$ to 9 at 2 years. nd, not determined. *KO group significantly different from age-matched WT group, $P < 0.05$.

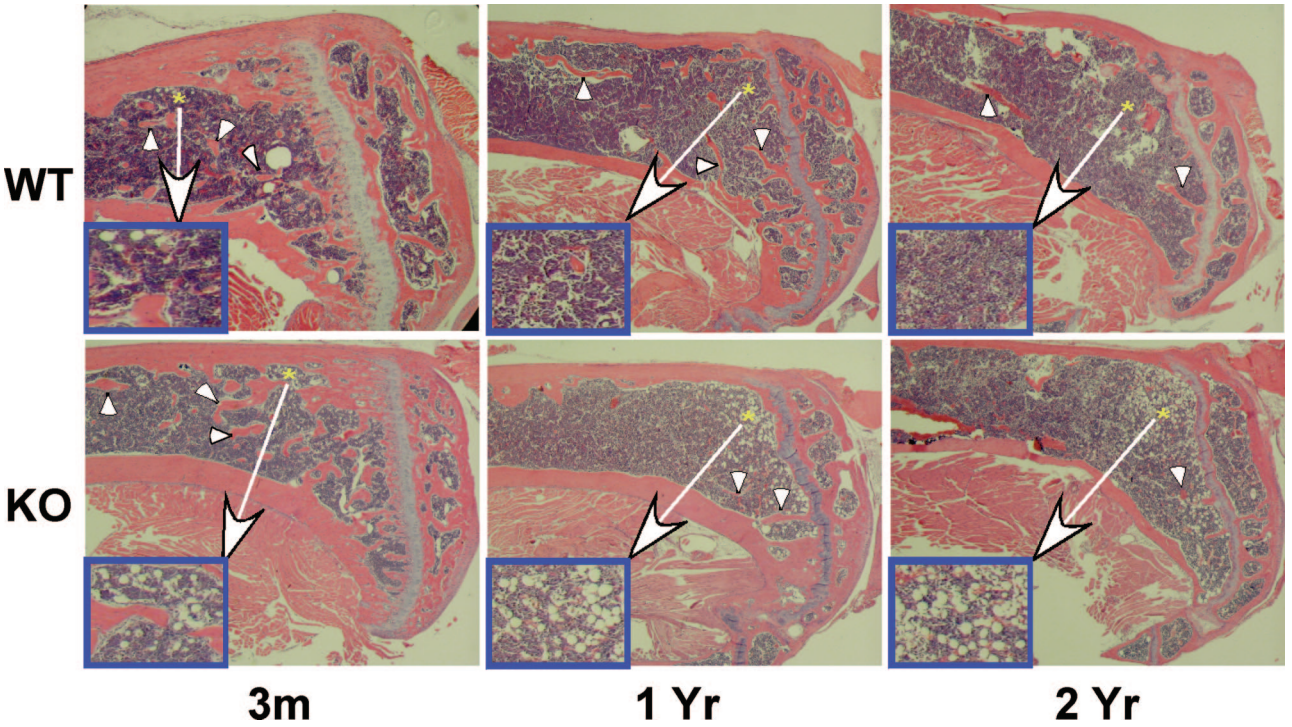

Figure 6. Histological evidence for increased fat deposition in KO mice. Longitudinal sections (10 μm) of decalcified tibiae from WT and iPLA$_2\beta$-null mice were stained with H&E and images captured with a Nikon camera. **Arrows** indicate trabecular network and **asterisk** indicate areas of fat accumulation (**insets**). Original magnifications: ×3; ×15 (**insets**).

WT mice with aging, is evident in H&E-stained sections (Figure 6). A closer examination of these sections reveals a near absence of fat accumulation in the bone marrow of WT mice (insets on the left side of each panel) but an age-related increase in bone marrow fat content in KO mice (3 months, 8.8 ± 2.4; 1 year, 17.5 ± 2.6; and 2 years, 31.8 ± 2.6 adipocytes/0.50 mm^2, 3 months versus 1 year, $P < 0.05$; 1 year versus 2 years, $P < 0.01$; 3 months versus 2 years, $P < 0.001$). In general, there is an inverse relationship between BMD and bone marrow fat,[29] and we observe an age-related decrease in the BMD of KO mice. These findings raise the possibility that osteoblasts are being replaced with adipocytes in the bone marrow of iPLA$_2\beta$-null mice.

BMSCs from KO Mice Express No iPLA$_2\beta$, Higher PPARγ, and Lower Runx2 Message

In view of the accumulation of fat in the bone marrow of KO mice, BMSCs were prepared from WT and KO mice to compare expression of transcription factors *PPARγ* and *Runx2,* which are required for adipocyte and osteoblast differentiation, respectively. As shown in Figure 7, BMSCs from WT but not KO mice express iPLA$_2$ β mRNA. Interestingly, *PPARγ* expression is increased and that of *Runx2* decreased in KO cells, relative to WT cells. Because osteoblasts and adipocytes have a common mesenchymal stem cell origin, these findings suggest that progenitor cells in KO mice have an apparent higher predisposition to differentiate into adipocytes and a lower predisposition to differentiate into osteoblasts.

Cultured BMSCs from KO Mice Exhibit Increased Adipogenesis and Decreased Osteogenesis

To examine the possibility of dysregulated BMSC differentiation in the KO mice, BMSCs prepared from WT and KO mice were stimulated with either an adipogenic or osteogenic medium. In support of the findings of higher *PPARγ* expression in undifferentiated KO-BMSCs, after exposure to an adipogenic medium, a significantly ($P <$

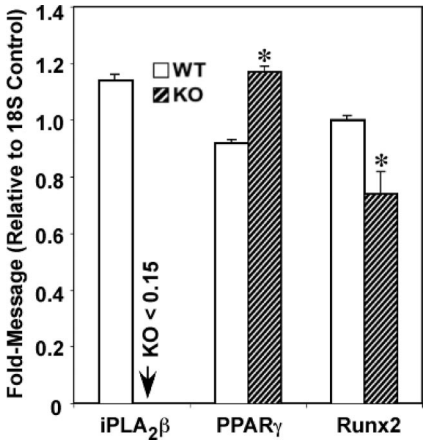

Figure 7. Adipogenic and osteogenic transcription factor expression in BMSCs. Pooled BMSCs were prepared from femora and tibiae of 3-month WT and iPLA$_2\beta$-null mice and cultured for 10 days. Total RNA was then isolated from the cells and processed for real-time PCR analyses of *PPARγ* and *Runx2*. The data represent mean ± SEM, where $n = 3$ to 6 in each group. KO group significantly different from WT group, $^*P < 0.05$.

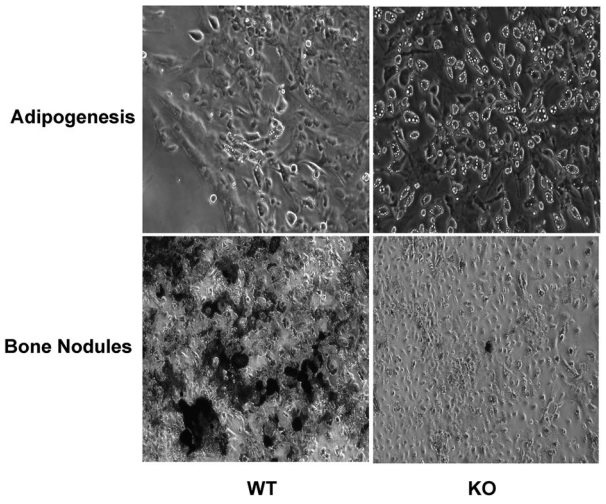

Figure 8. *Ex vivo* adipogenesis and bone nodule formation in BMSCs. Pooled BMSCs were prepared as in Figure 7 and cultured for 10 days. The media was then changed to either an adipogenic or osteogenic medium. Images of fat deposition were obtained on day 4 and bone nodule formation was visualized using von Kossa stain on day 9. Original magnifications, ×10.

0.0001) higher abundance of cells with fat deposits is evident in the KO-BMSCs (95 ± 2% of total cells) compared to the WT-BMSCs (11 ± 3% of total cells) (Figure 8). And, as suggested by lower *Runx2* expression in undifferentiated KO-BMSCs, bone nodule formation, reflected by von Kossa (black) staining of mineralizing bone, is significantly more prominent in the WT-BMSCs than in KO-BMSCs exposed to an osteogenic medium. These findings support the hypothesis that in the absence of iPLA$_2\beta$, there is a shift in the lineage determination of progenitor cells to differentiate into adipocytes at the expense of differentiating into osteoblasts.

Discussion

PGs and other bioactive eicosanoids are involved in maintaining normal bone health and structure.[30–32] The PGs are generated via COX-catalyzed metabolism of AA after its hydrolysis from membrane phospholipids by phospholipases A_2 (PLA$_2$s). Studies to date have focused on the roles of cPLA$_2$ and sPLA$_2$ in regulating bone metabolism and they demonstrated that bone resorption induced by PTH,[33] cadmium,[34] or lipopolysaccharide[6] is associated with activation of cPLA$_2$ and bone resorption induced by interleukin (IL)-1[35] or ovariectomy[36] with activation of sPLA$_2$. Further, they reported that bone loss attributable to inflammation is prevented in cPLA$_2$-null mice, whereas that due to a decrease in estrogen is suppressed by sPLA$_2$ inhibitors. These observations suggest that cPLA$_2$ and sPLA$_2$ participate in bone resorption induced by certain stimuli. However, no temporal relationship between PLA$_2$ activation and PGE2 synthesis throughout the course of reduced osteoid mineralization was evident.[37] In addition, inhibition of COX-2 by indomethacin did not prevent IL-1-induced decrease in mineralization.[35] These findings reveal that other products of AA metabolism (ie, leukotrienes, HETEs, PAF)[1,38] participate in bone resorption.

Here, we demonstrate that iPLA$_2\beta$ mRNA is expressed in bones from WT mice but not in bones from iPLA$_2\beta$-null mice, and that aging iPLA$_2\beta$-null mice exhibit lower whole body BMD, accelerated loss of cortical and trabecular bone, impaired bone mechanical properties, increases in bone marrow fat (BMF) content, and dysregulation of adipogenic and osteogenic transcription factors that are reflected by increased adipogenesis and decreased bone nodule formation. These observations provide the first evidence that iPLA$_2\beta$ is required for maintenance of normal bone metabolism and mass.

We observed an increase in BMD in WT mice between 3 months and 1 year, which is consistent with previous reports that BMD increases with age until peak bone mass is reached (at ~1 year).[39–41] In contrast, we observe no such increase in BMD in iPLA$_2\beta$-null mice. One possibility is that differences in the WT and KO bones might be related to the lower BW recorded in the older KO mice. However, the BW in the 2-year-old iPLA$_2\beta$-null group was similar to that in both WT and iPLA$_2\beta$-null groups at 3 months, although a similar low bone mass phenotype is not evident in the 3-month-old iPLA$_2\beta$-null mice; calcein labeling in the iPLA$_2\beta$-null mice demonstrates abnormal bone formation rate; and iPLA$_2\beta$-null mice have higher bone marrow fat and exhibit dysregulated BMSC differentiation. The data, when considered collectively, suggest that the low bone mass phenotype exhibited by the iPLA$_2\beta$-null mice cannot be accounted for by a decrease in BW. We therefore considered other possibilities that could cause a low bone mass phenotype in the absence of iPLA$_2\beta$.

Maintenance of bone health and structure is dependent on the opposing processes of bone resorption and bone formation. As in humans,[42–44] decreases in bone volume and trabecular number are part of the natural aging process in C57BL/6 mice,[45–48] and our histology and μCT analyses indicate that the abnormal bone phenotype in iPLA$_2\beta$-null mice is accelerated in the absence of iPLA$_2\beta$. Examination of bone resorption parameters reveal no accompanying increase in osteoclast abundance or activity, suggesting that bone resorption, most likely is not responsible for bone loss in iPLA$_2\beta$-null mice. Bone loss in iPLA$_2\beta$-null mice was also not associated with changes in circulating levels of estradiol, follicle-stimulating hormone, and amylin, or with renal function, all known to impact bone modeling. In addition, we have previously reported that female iPLA$_2\beta$-null mice in the age range studied here have normal glucose and insulin levels and glucose tolerance.[14] However, calcein labeling, a gold-standard measure of active bone mineralizing surface, is reduced in periosteal bone and is profoundly attenuated in endocortical (Ec) bone from KO mice. MS/BS and MAR are also significantly reduced in KO mice. These findings suggest that a decrease in osteoblast function contributes to the low bone mass phenotype in iPLA$_2\beta$-null mice. This possibility is supported by the findings that iPLA$_2\beta$ mRNA is more abundant in bone-forming osteoblast cells than in osteoclast cells involved in bone resorption.

Lower bone volumes in the KO mice are also associated with a decrease in bone strength reflected by whole-bone mechanical testing. The changes in ultimate and yield moments, rigidity, and energy to fracture from 3 months to 2 years all reflect a relative decline in mechanical properties in femora from KO mice versus WT controls. These decreases are consistent with the relative differences in cross-sectional morphology of the femoral diaphysis, as reflected by diminished bone area and moment of inertia in KO mice with aging. Taken together, these data indicate that although iPLA$_2\beta$-null mice develop inferior bone mechanical properties with age, the properties are appropriate to their size, and we find no evidence of a material level defect. The lack of difference in post-yield displacement (a measure of brittleness) between WT and KO bones supports this conclusion.

Curiously, fat accumulates to a greater degree with age in the bone marrow of KO mice compared to WT mice. Interestingly, an inverse relationship between BMF content and BMD has been reported in humans with osteoporosis,[29,49,50] and older KO mice have lower BMD than age-matched WT mice in our study. Because osteoblasts and adipocytes share a common mesenchymal stem cell origin, the increase in BMF content in KO mice might be caused by dysregulation of differentiation in the absence of iPLA$_2\beta$. Differentiation of BMSCs into osteoblasts is regulated by transcription factor *Runx2* and into adipocytes by transcription factor *PPAR*γ.[51,52] and we find that expression of *PPAR*γ is increased and of *Runx2* decreased in undifferentiated BMSCs prepared from the KO mice. These findings raise the possibility that BMSCs in KO mice have a greater predisposition to differentiate into adipocytes and a lesser predisposition to differentiate into osteoblasts. This in fact appears to be so, because we find that when BMSCs harvested from WT and KO mice are cultured in osteogenesis media, more bone nodules form from WT cells, but when cultured in adipogenic medium much greater adipogenesis is evident in KO cells.

Collectively, our data indicate that absence of iPLA$_2\beta$ leads to lower bone mass and that decreases in osteoblast function and dysregulation of BMSC differentiation contribute to this phenotype. It might be speculated that iPLA$_2\beta$ and/or products of its activation participate in these pathways and that their absence either shifts the balance from osteoblast formation toward adipocyte formation or eliminates stimuli necessary for differentiation of BMSCs to osteoblasts. Several reports indicate that products of PLA$_2$, such as AA and PGE2, have positive effects on bone formation. For instance, supplementation of diets fed to piglets with AA increased whole body and BMD[7] and bone mass[53,54] and decreased bone resorption.[55] Other studies implicate PGE2 as the mediator of AA-induced bone formation. Among the bone-modeling cells, PGE2 is produced mainly by osteoblasts[56,57] and has been reported to enhance bone formation at low doses but increase bone resorption at high doses.[2–6] The differential effects of PGE2 are attributed to the presence of multiple cell-surface PG receptors.[58–63] Systemic or local injections of PGE2 have also been shown to stimulate bone formation in rats[2,62] and in piglets,[55] and reduce bone loss in rats attributable to disuse or orchidectomy.[5,64,65] Additionally, lamellar bone formation in response to mechanical strain is mediated by COX-2[30,66] and COX-2$^{-/-}$ mice have decreased bone density.[67]

Further, PGE2 induces bone nodules to form in BMSC cultures[2,68] and in cultured calvaria osteoblasts[69–72] and osteoblastogenesis from bone marrow precursors.[73] BMSCs isolated from rats injected with PGE2 for 2 weeks produce four times more mineralized bone nodules than control BMSCs.[73] PGE2 increases bone nodule formation in low-density cultures of rat bone marrow cells by recruiting osteoblast precursors present in the bone marrow.[74] Collectively, these findings suggest that PGE2 participates in bone formation. The demonstration that PGE2 enhances bone morphogenetic protein-induced osteoblastogenesis and expression of *Runx2/cbfa1* and *osterix*,[63] which are required for osteoblast differentiation, suggests a potential mechanism by which PGE2 can contribute to bone formation.

PGE2 produces its effects through its interaction with four recognized PGE2 receptor subtypes (EP1 to EP4), that differ in the signal transduction pathway they trigger.[75–78] *In vitro*[68,79] and *in vivo*[80,81] studies suggest that the bone anabolic effects of PGE2 are mediated through the EP4 receptor. Further, an EP4 receptor-selective PGE2 agonist was reported to stimulate cortical bone formation and restore bone mass and strength in aged OVX rats.[82] Mesenchymal stem cells express COX-2 and EP4 receptors and constitutively synthesize PGE2.[58] The secreted PGE2 has been shown to activate the EP4 receptor leading to induction *of Runx2/cbaf1* and *osterix*[81] and BMP2,[58] which are all essential for bone formation. EP4 receptor is also expressed by preadipocyte cells,[83] and activation of this receptor by PGE2 suppresses induction of adipogenesis marker gene peroxisome proliferator-activated receptor gamma (*PPAR*γ) and inhibits adipocyte differentiation.[83,84] An EP4 antagonist or inhibition of COX-2, however, promotes adipocyte differentiation. PGE2 also has been demonstrated to decrease fatty marrow area in the proximal tibial metaphysis of aged rats.[85] Collectively, these observations reveal a dual role for PGE2; in increasing bone formation and decreasing adipogenesis, giving rise to the strong possibility that reduced generation of PGE2, as would be expected in the absence of iPLA$_2\beta$, contributes to decreased osteogenesis and increased bone marrow adipogenesis.

Additional regulators of osteoblast differentiation that could be affected by an absence of iPLA$_2\beta$ include regulator of G protein signaling (RGS2) and oxysterols. Osteoblast differentiation is promoted by RGS2,[86] and iPLA$_2\beta$ stimulates transcriptional up-regulation of RGS2 in response to incubating vascular smooth muscle cells with angiotensin II.[54] This transcriptional up-regulation is blocked by pharmacological inhibition of iPLA$_2\beta$ with BEL and does not occur in iPLA$_2\beta$-null vascular smooth muscle cells.[87] Oxysterols are naturally occurring cholesterol oxidation products that regulate differentiation of mesenchymal stem cells to promote osteogenesis and inhibit adipogenesis.[88–90] COX products participate in osteogenesis, and this is blocked by iPLA$_2\beta$ inhibitors.[89]

Collectively, our findings indicate that iPLA$_2\beta$ contributes to maintenance of bone mass and that its role becomes more important with age. Another factor that contributes to age-related bone loss is the accumulation of fat cells in the bone marrow,[91] and this is accentuated in iPLA$_2\beta$-null mice. The observations that the onset of higher bone marrow adipogenesis and reduced trabecular MAR is evident in the 3-month KO mice suggests that bone abnormalities attributable to an absence in iPLA$_2\beta$ begin to emerge by this age. Our findings therefore suggest that iPLA$_2\beta$ might be an important regulator of bone formation and BMSC differentiation. However, although renal function and the levels of circulating glucose, insulin, and several other factors that can affect bone modeling are not altered in the iPLA$_2\beta$-null mice, the possibility that metabolic abnormalities, as yet unrecognized, could contribute to the bone phenotype in the absence of iPLA$_2\beta$ cannot be completely eliminated.

Acknowledgments

We thank Ms. Min Tan, Mr. Wu Jin, Mr. Samuel Smith, and Ms. Michelle Lynch for their expert technical assistance; Ms. Crystal Idelburg for histological processing; Dr. Shunzhong Bao and Dr. Manu Chakravarthy for designing PCR primers; Dr. Trey Coleman for assistance with the DEXA analyses; Mr. Brian Uthgenannt for assistance with the μCT analyses; Mr. G. Wade Sherrow for performing the plasma assays; and Dr. Dwight Towler, Dr. Roberto Civitelli, and Dr. Steven Teitelbaum for helpful discussions.

References

1. Traianedes K, Dallas MR, Garrett IR, Mundy GR, Bonewald LF: 5-Lipoxygenase metabolites inhibit bone formation in vitro. Endocrinology 1998, 139:3178–3184
2. Weinreb M, Suponitzky I, Keila S: Systemic administration of an anabolic dose of PGE2 in young rats increases the osteogenic capacity of bone marrow. Bone 1997, 20:521–526
3. Yang RS, Liu TK, Lin-Shiau SY: Increased bone growth by local prostaglandin E2 in rats. Calcif Tissue Int 1993, 52:57–61
4. Weinreb M, Shamir D, Machwate M, Rodan GA, Harada S, Keila S: Prostaglandin E2 (PGE2) increases the number of rat bone marrow osteogenic stromal cells (BMSC) via binding the EP4 receptor, activating sphingosine kinase and inhibiting caspase activity. Prostaglandins Leukot Essen Fatty Acids 2006, 75:81–90
5. Akamine T, Jee WS, Ke HZ, Li XJ, Lin BY: Prostaglandin E2 prevents bone loss and adds extra bone to immobilized distal femoral metaphysis in female rats. Bone 1992, 13:11–22
6. Miyaura C, Inada M, Matsumoto C, Ohshiba T, Uozumi N, Shimizu T, Ito A: An essential role of cytosolic phospholipase A2α in prostaglandin E2-mediated bone resorption associated with inflammation. J Exp Med 2003, 197:1303–1310
7. Weiler HA: Dietary supplementation of arachidonic acid is associated with higher whole body weight and bone mineral density in growing pigs. Pediatr Res 2000, 47:692–697
8. Sato Y, Arai N, Negishi A, Ohya K: Expression of cyclooxygenase genes and involvement of endogenous prostaglandin during osteogenesis in the rat tibial bone marrow cavity. J Med Dent Sci 1997, 44:81–92
9. Smith WL: The eicosanoids and their biochemical mechanisms of action. Biochem J 1989, 259:315–324
10. Schaloske RH, Dennis EA: The phospholipase A$_2$ superfamily and its group numbering system. Biochim Biophys Acta–Mol Cell Biol Lipid 2006, 1761:1246–1259
11. Murphy R, Sala A: Quantitation of sulfidopeptide leukotrienes in biological fluids by gas chromatography-mass spectrometry. Methods Enzymol 1990, 187:90–98
12. Turk J, Ramanadham S: The expression and function of a group VIA calcium-independent phospholipase A$_2$ (iPLA$_2\beta$) in beta-cells. Can J Physiol Pharmacol 2004, 82:824–832
13. Bao S, Miller DJ, Ma Z, Wohltmann M, Eng G, Ramanadham S, Moley K, Turk J: Male mice that do not express group VIA phospholipase A$_2$ produce spermatozoa with impaired motility and have greatly reduced fertility. J Biol Chem 2004, 279:38194–38200
14. Bao S, Song H, Wohltmann M, Ramanadham S, Jin W, Bohrer A, Turk J: Insulin secretory responses and phospholipid composition of pancreatic islets from mice that do not express group via phospholipase A$_2$ and effects of metabolic stress on glucose homeostasis. J Biol Chem 2006, 281:20958–20973
15. Moran JM, Buller RML, McHowat J, Turk J, Wohltmann M, Gross RW, Corbett JA: Genetic and pharmacologic evidence that calcium-independent phospholipase A$_2\beta$ regulates virus-induced inducible nitric-oxide synthase expression by macrophages. J Biol Chem 2005, 280:28162–28168
16. Larsson PKA, Claesson H-E, Kennedy BP: Multiple splice variants of the human calcium-independent phospholipase A$_2$ and their effect on enzyme activity. J Biol Chem 1998, 273:207–214
17. Ma Z, Zhang S, Turk J, Ramanadham S: Stimulation of insulin secretion and associated nuclear accumulation of iPLA$_2\beta$ in INS-1 insulinoma cells. Am J Physiol 2002, 282:E820–E833
18. Castro CH, Shin CS, Stains JP, Cheng SL, Sheikh S, Mbalaviele G, Szejnfeld VL, Civitelli R: Targeted expression of a dominant-negative N-cadherin in vivo delays peak bone mass and increases adipogenesis. J Cell Sci 2004, 117:2853–2864
19. Novack DV, Yin L, Hagen-Stapleton A, Schreiber RD, Goeddel DV, Ross FP, Teitelbaum SL: The κB function of NFκB2 p100 controls stimulated osteoclastogenesis. J Exp Med 2003, 198:771–781
20. Christiansen BA, Silva MJ: The effect of varying magnitudes of whole-body vibration on several skeletal sites in mice. Ann Biomed Eng 2006, 34:1149–1156
21. Silva MJ, Brodt MD, Wopenka B, Thomopoulos S, Williams D, Wassen MHM, Ko M, Kusano N, Bank RA: Decreased collagen organization and content are associated with reduced strength of demineralized and intact bone in the SAMP6 mouse. J Bone Miner Res 2006, 21:78–88
22. Hilton MJ, Tu X, Long F: Tamoxifen-inducible gene deletion reveals a distinct cell type associated with trabecular bone, and direct regulation of PTHrP expression and chondrocyte morphology by Ihh in growth region cartilage. Dev Biol 2007, 308:93–105
23. Tu X, Joeng KS, Nakayama KI, Nakayama K, Rajagopal J, Carroll TJ, McMahon AP, Long F: Noncanonical Wnt signaling through G protein-linked PKCδ activation promotes bone formation. Dev Cell 2007, 12:113–127
24. Bianco P, Riminucci M, Gronthos S, Robey PG: Bone marrow stromal stem cells: nature, biology, and potential applications. Stem Cells 2001, 19:180–192
25. Riggs BL, Jowsey J, Goldsmith RS, Kelly PJ, Hoffman DL, Arnaud CD: Short- and long-term effects of estrogen and synthetic anabolic hormone in postmenopausal osteoporosis. J Clin Invest 1972, 51:1659-1663
26. Iqbal J, Sun L, Kumar TR, Blair HC, Zaidi M: Follicle-stimulating hormone stimulates TNF production from immune cells to enhance osteoblast and osteoclast formation. Proc Natl Acad Sci USA 2006, 103:14925–14930
27. Dacquin R, Davey RA, Laplace C, Levasseur R, Morris HA, Goldring SR, Gebre-Medhin S, Galson DL, Zajac JD, Karsenty G: Amylin inhibits bone resorption while the calcitonin receptor controls bone formation in vivo. J Cell Biol 2004, 164:509–514
28. Julian BA, Laskow DA, Dubovsky J, Dubovsky EV, Curtis JJ, Quarles LD: Rapid loss of vertebral mineral density after renal transplantation. N Engl J Med 1991, 325:544–550
29. Schellinger D, Lin CS, Lim J, Hatipoglu HG, Pezzullo JC, Singer AJ: Bone marrow fat and bone mineral density on proton MR spectroscopy and dual-energy x-ray absorptiometry: their ratio as a new indicator of bone weakening. Am J Roentgenol 2004, 183:1761–1765
30. Forwood MR: Inducible cyclo-oxygenase (COX-2) mediates the in-

duction of bone formation by mechanical loading in vivo. J Bone Miner Res 1996, 11:168–169
31. Okada Y, Lorenzo JA, Freeman AM, Tomita M, Morham SG, Raisz LG, Pilbeam CC: Prostaglandin G/H synthase-2 is required for maximal formation of osteoclast-like cells in culture. J Clin Invest 2000, 105:823–832
32. Li M, Thompson D, Paralkar V: Prostaglandin E2 receptors in bone formation. Int Orthop 2007, 31:767–772
33. MacDonald BR, Gallagher JA, Ahnfelt-Ronne I, Beresford JN, Gowen M, Russell RG: Effects of bovine parathyroid hormone and 1,25-dihydroxyvitamin D3 on the production of prostaglandins by cells derived from human bone. FEBS Lett 1984, 169:49–52
34. Miyahara T, Tonoyama H, Watanabe M, Okajima A, Miyajima S, Sakuma T, Nemoto N, Takayama K: Stimulative effect of cadmium on prostaglandin E2 production in primary mouse osteoblastic cells. Calcif Tissue Int 2001, 68:185–191
35. Ellies LG, Heersche JN, Pruzanski W, Vadas P, Aubin JE: The role of phospholipase A_2 in interleukin-1 alpha-mediated inhibition of mineralization of the osteoid formed by fetal rat calvaria cells in vitro. J Dent Res 1993, 72:18–24
36. Gregory LS, Kelly WL, Reid RC, Fairlie DP, Forwood MR: Inhibitors of cyclo-oxygenase-2 and secretory phospholipase A_2 preserve bone architecture following ovariectomy in adult rats. Bone 2006, 39:134–142
37. Ellies LG, Heersche JN, Vadas P, Pruzanski W, Stefanski E, Aubin JE: Interleukin-1 alpha stimulates the release of prostaglandin E2 and phospholipase A_2 from fetal rat calvarial cells in vitro: relationship to bone nodule formation. J Bone Miner Res 1991, 6:843–850
38. Meghji S, Sandy JR, Scutt AM, Harvey W, Harris M: Stimulation of bone resorption by lipoxygenase metabolites of arachidonic acid. Prostaglandins 1988, 36:139–149
39. Bhattacharya A, Rahman M, Sun D, Fernandes G: Effect of fish oil on bone mineral density in aging C57BL/6 female mice. J Nutr Biochem 2007, 18:372–379
40. Hamrick MW, Ding K-H, Pennington C, Chao YJ, Wu Y-D, Howard B, Immel D, Borlongan C, McNeil PL, Bollag WB: Age-related loss of muscle mass and bone strength in mice is associated with a decline in physical activity and serum leptin. Bone 2006, 39:845–853
41. Nieminen J, Sahlman J, Hirvonen T, Jamsa T, Tuukkanen J, Kovanen V, Kroger H, Jurvelin J, Arita M, Li SW, Prockop DJ, Hyttinen MM, Helminen HJ, Lapvetelainen T, Puustjarvi K: Abnormal response to physical activity in femurs after heterozygous inactivation of one allele of the Col2a1 gene for type II collagen in mice. Calcif Tissue Int 2005, 77:104–112
42. Feik SA, Thomas CD, Clement JG: Age-related changes in cortical porosity of the midshaft of the human femur. J Anat 1997, 191:407–416
43. Overton TR, Basu TK: Longitudinal changes in radial bone density in older men. Eur J Clin Nutr 1999, 53:211–215
44. Parfitt AM: Age-related structural changes in trabecular and cortical bone: cellular mechanisms and biomechanical consequences. Calcif Tissue Int 1984, 36:S123–S128
45. Cao J, Venton L, Sakata T, Halloran BP: Expression of RANKL and OPG correlates with age-related bone loss in male C57BL/6 mice. J Bone Miner Res 2003, 18:270–277
46. Ferguson VL, Ayers RA, Bateman TA, Simske SJ: Bone development and age-related bone loss in male C57BL/6J mice. Bone 2003, 33:387–398
47. Halloran BP, Ferguson VL, Simske SJ, Burghardt A, Venton LL, Majumdar S: Changes in bone structure and mass with advancing age in the male C57BL/6J mouse. J Bone Miner Res 2002, 17:1044–1050
48. Ke HZ, Brown TA, Qi H, Crawford DT, Simmons HA, Petersen DN, Allen MR, McNeish JD, Thompson DD: The role of estrogen receptor-beta, in the early age-related bone gain and later age-related bone loss in female mice. J Musculoskel Neurol Interact 2002, 2:479–488
49. Griffith JF, Yeung DKW, Antonio GE, Lee FKH, Hong AWL, Wong SYS, Lau EMC, Leung PC: Vertebral bone mineral density, marrow perfusion, and fat content in healthy men and men with osteoporosis: dynamic contrast-enhanced MR imaging and MR spectroscopy. Radiology 2005, 236:945–951
50. Yeung DKW, Griffith JF, Antonio GE, Lee FKH, Woo J, Leung PC: Osteoporosis is associated with increased marrow fat content and decreased marrow fat unsaturation: a proton MR spectroscopy study. J Magn Reson Imaging 2005, 22:279–285
51. Pittenger MF, Mackay AM, Beck SC, Jaiswal RK, Douglas R, Mosca JD, Moorman MA, Simonetti DW, Craig S, Marshak DR: Multilineage potential of adult human mesenchymal stem cells. Science 1999, 284:143–147
52. Hong J-H, Hwang ES, McManus MT, Amsterdam A, Tian Y, Kalmukova R, Mueller E, Benjamin T, Spiegelman BM, Sharp PA, Hopkins N, Yaffe MB: TAZ, a transcriptional modulator of mesenchymal stem cell differentiation. Science 2005, 309:1074–1078
53. Blanaru JL, Kohut JR, Fitzpatrick-Wong SC, Weiler HA: Dose response of bone mass to dietary arachidonic acid in piglets fed cow milk-based formula. Am J Clin Nutr 2004, 79:139–147
54. Mollard RC, Kovacs HR, Fitzpatrick-Wong SC, Weiler HA: Low levels of dietary arachidonic and docosahexaenoic acids improve bone mass in neonatal piglets, but higher levels provide no benefit. J Nutr 2005, 135:505–512
55. Lucia VD, Fitzpatrick-Wong SC, Weiler HA: Dietary arachidonic acid suppresses bone turnover in contrast to low dosage exogenous prostaglandin E2 that elevates bone formation in the piglet. Prostaglandins Leukot Essent Fatty Acids 2003, 68:407–413
56. Chen Q-R, Miyaura C, Higashi S, Murakami M, Kudo I, Saito S, Hiraide T, Shibasaki Y, Suda T: Activation of cytosolic phospholipase A_2 by platelet-derived growth factor is essential for cyclooxygenase-2-dependent prostaglandin E2 synthesis in mouse osteoblasts cultured with interleukin-1. J Biol Chem 1997, 272:5952–5958
57. Tai H, Miyaura C, Pilbeam CC, Tamura T, Ohsugi Y, Koishihara Y, Kubodera N, Kawaguchi H, Raisz LG, Suda T: Transcriptional induction of cyclooxygenase-2 in osteoblasts is involved in interleukin-6-induced osteoclast formation. Endocrinology 1997, 138:2372–2379
58. Arikawa T, Omura K, Morita I: Regulation of bone morphogenetic protein-2 expression by endogenous prostaglandin E2 in human mesenchymal stem cells. J Cell Physiol 2004, 200:400–406
59. Okada Y, Pilbeam C, Raisz L, Tanaka Y: Role of cyclooxygenase-2 in bone resorption. J Uoeh 2003, 25:185–195
60. Kasugai S, Oida S, Iimura T, Arai N, Takeda K, Ohya K, Sasaki S: Expression of prostaglandin E receptor subtypes in bone: expression of EP2 in bone development. Bone 1995, 17:1–4
61. Mo A, Yao W, Li C, Tian X, Su M, Ling Y, Zhang Q, Setterberg RB, Jee WSS: Bipedal stance exercise and prostaglandin E2 (PGE2) and its synergistic effect in increasing bone mass and in lowering the PGE2 dose required to prevent ovariectomized-induced cancellous bone loss in aged rats. Bone 2002, 31:402–406
62. Suponitzky I, Weinreb M: Differential effects of systemic prostaglandin E2 on bone mass in rat long bones and calvariae. J Endocrinol 1998, 156:51–57
63. Zhang X, Schwarz EM, Young DA, Puzas JE, Rosier RN, O'Keefe RJ: Cyclooxygenase-2 regulates mesenchymal cell differentiation into the osteoblast lineage and is critically involved in bone repair. J Clin Invest 2002, 109:1405–1415
64. Jee WS, Akamine T, Ke HZ, Li XJ, Tang LY, Zeng QQ: Prostaglandin E2 prevents disuse-induced cortical bone loss. Bone 1992, 13:153–159
65. Li M, Jee WS, Ke HZ, Tang LY, Ma YF, Liang XG, Setterberg RB: Prostaglandin E2 administration prevents bone loss induced by orchidectomy in rats. J Bone Miner Res 1995, 10:66–73
66. Duncan RL, Turner CH: Mechanotransduction and the functional response of bone to mechanical strain. Calcif Tissue Int 1995, 57:344–358
67. Xu Z, Choudhary S, Okada Y, Voznesensky O, Alander C, Raisz L, Pilbeam C: Cyclooxygenase-2 gene disruption promotes proliferation of murine calvarial osteoblasts in vitro. Bone 2007, 41:68–76
68. Weinreb M, Grosskopf A, Shir N: The anabolic effect of PGE2 in rat bone marrow cultures is mediated via the EP4 receptor subtype. Am J Physiol 1999, 276:E376–E383
69. Nagata T, Kaho K, Nishikawa S, Shinohara H, Wakano Y, Ishida H: Effect of prostaglandin E2 on mineralization of bone nodules formed by fetal rat calvarial cells. Calcif Tissue Int 1994, 55:451–457
70. Flanagan AM, Chambers TJ: Stimulation of bone nodule formation in vitro by prostaglandins E1 and E2. Endocrinology 1992, 130:443–448
71. Kaneki H, Takasugi I, Fujieda M, Kiriu M, Mizuochi S, Ide H: Prostaglandin E2 stimulates the formation of mineralized bone nodules by a cAMP-independent mechanism in the culture of adult rat calvarial osteoblasts. J Cell Biochem 1999, 73:36–48
72. Tang LY, Kimmel DB, Jee WS, Yee JA: Functional characterization of prostaglandin E2 inducible osteogenic colony forming units in cul-

tures of cells isolated from the neonatal rat calvarium. J Cell Physiol 1996, 166:76–83
73. Keila S, Kelner A, Weinreb M: Systemic prostaglandin E2 increases cancellous bone formation and mass in aging rats and stimulates their bone marrow osteogenic capacity in vivo and in vitro. J Endocrinol 2001, 168:131–139
74. Scutt A, Zeschnigk M, Bertram P: PGE2 induces the transition from non-adherent to adherent bone marrow mesenchymal precursor cells via a cAMP/EP2-mediated mechanism. Prostaglandins 1995, 49:383–395
75. Narumiya S, Sugimoto Y, Ushikubi F: Prostanoid receptors: structures, properties, and functions. Physiol Rev 1999, 79:1193–1226
76. Sugimoto Y, Narumiya S, Ichikawa A: Distribution and function of prostanoid receptors: studies from knockout mice. Prog Lipid Res 2000, 39:289–314
77. Breyer RM, Bagdassarian CK, Myers SA, Breyer MD: Prostanoid receptors: subtypes and signaling. Annu Rev Pharmacol Toxicol 2001, 41:661–690
78. Negishi M, Sugimoto Y, Ichikawa A: Prostaglandin E receptors. J Lipid Mediat Cell Signal 1995, 12:379–391
79. Raisz LG, Woodiel FN: Effects of selective prostaglandin EP2 and EP4 receptor agonists on bone resorption and formation in fetal rat organ cultures. Prostaglandins Other Lipid Mediat 2003, 71:287–292
80. Machwate M, Harada S, Leu CT, Seedor G, Labelle M, Gallant M, Hutchins S, Lachance N, Sawyer N, Slipetz D, Metters KM, Rodan SB, Young R, Rodan GA: Prostaglandin receptor EP4 mediates the bone anabolic effects of PGE2. Mol Pharmacol 2001, 60:36–41
81. Yoshida K, Oida H, Kobayashi T, Maruyama T, Tanaka M, Katayama T, Yamaguchi K, Segi E, Tsuboyama T, Matsushita M, Ito K, Ito Y, Sugimoto Y, Ushikubi F, Ohuchida S, Kondo K, Nakamura T, Narumiya S: Stimulation of bone formation and prevention of bone loss by prostaglandin E EP4 receptor activation. Proc Natl Acad Sci USA 2002, 99:4580–4585
82. Ke HZ, Crawford DT, Qi H, Simmons HA, Owen TA, Paralkar VM, Li M, Lu B, Grasser WA, O Cameron K, Lefker BA, DaSilva-Jardine P, O Scott DO, Zhang Q, Tian XY, Jee WSS, Brown TA, Thompson D: A nonprostanoid EP4 receptor selective prostaglandin E2 agonist restores bone mass and strength in aged, ovariectomized rats. J Bone Miner Res 2006, 21:565–575
83. Tsuboi H, Sugimoto Y, Kainoh T, Ichikawa A: Prostanoid EP4 receptor is involved in suppression of 3T3–L1 adipocyte differentiation. Biochem Biophys Res Commun 2004, 322:1066–1072
84. Sugimoto Y, Tsuboi H, Okuno Y, Tamba S, Tsuchiya S, Tsujimoto G, Ichikawa A: Microarray evaluation of EP4 receptor-mediated prostaglandin E2 suppression of 3T3–L1 adipocyte differentiation. Biochem Biophys Res Commun 2004, 322:911–917
85. Cui L, Ma YF, Yao W, Zhou H, Setterberg RB, Liang TC, Jee WSS: Cancellous bone of aged rats maintains its capacity to respond vigorously to the anabolic effects of prostaglandin E2 by modeling-dependent bone gain. J Bone Miner Metab 2001, 19:29–37
86. Roy AA, Nunn C, Ming H, Zou M-X, Penninger J, Kirshenbaum LA, Dixon SJ, Chidiac P: Up-regulation of endogenous RGS2 mediates cross-desensitization between Gs and Gq signaling in osteoblasts. J Biol Chem 2006, 281:32684–32693
87. Xie Z, Gong MC, Su W, Turk J, Guo Z: Group VIA phospholipase A_2 (iPLA$_2\beta$) participates in angiotensin II-induced transcriptional up-regulation of RGS2 in vascular smooth muscle cells. J Biol Chem 2007, 282:25278–25289
88. Shouhed D, Kha HT, Richardson JA, Amantea CM, Hahn TJ, Parhami F: Osteogenic oxysterols inhibit the adverse effects of oxidative stress on osteogenic differentiation of marrow stromal cells. J Cell Biochem 2005, 95:1276–1283
89. Kha HT, Basseri B, Shouhed D, Richardson J, Tetradis S, Hahn TJ, Parhami F: Oxysterols regulate differentiation of mesenchymal stem cells: pro-bone and anti-fat. J Bone Miner Res 2004, 19:830–840
90. Aghaloo TL, Amantea CM, Cowan CM, Richardson JA, Wu BM, Parhami F, Tetradis S: Oxysterols enhance osteoblast differentiation in vitro and bone healing in vivo. J Orthop Res 2007, 25:1488–1497
91. Hamrick MW, Fera MAD, Choi Y-H, Hartzell D, Pennington C, Baile CA: Injections of leptin into rat ventromedial hypothalamus increase adipocyte apoptosis in peripheral fat and in bone marrow. Cell Tissue Res 2007, 327:133–141